Investigation of buffet control on transonic airfoil by tangential jet blowing

Abramova K.A., Brutyan M.A.***, Lyapunov S.V.**, Petrov A.V.**, Potapchik A.V.**, Ryzhov A.A.***, Soudakov V.G.***

**MIPT*

140180, Moscow region, Zhukovsky, Gagarin str., 16

*** TsAGI*

140180, Moscow region, Zhukovsky, Zhukovsky str., 1

Abstract

Two-dimensional steady-state and unsteady numerical simulations are carried out in the framework of Reynolds averaged Navier-Stokes equations to characterize the buffet phenomenon on supercritical transonic airfoil. Tangential jet blowing is investigated to delay buffet onset on the airfoil. In this case, the jet of compressed air is blown continuously from small slot nozzle tangentially to wing upper surface in the region of shock location to reduce shock-induced separation.

1. Introduction

The flight envelope of a civil transonic aircraft is limited by the buffet phenomenon associated with the separation under shock foot on the upper surface of the wing. Buffet results in lift and drag variations that greatly affect the aircraft aerodynamics. This phenomenon can further lead to structural vibrations (buffeting). Wing design standards impose margins between the buffeting onset and the cruise condition. As a consequence, a delay in buffeting onset could lead to improved aerodynamic performance characteristics that can lead to reduced wing area and then reduced friction drag and weight. One of the ways to delay buffet is the concept of flow control.

This problem is very close to the problem of the shock-boundary layer interaction (SBLI). In literature, there is a big variety of methods to control SBLI. One of the well-known passive methods is a cavity under shock foot covered with a perforated plate [1]. Other passive devices are grooves and stream-wise slots [2]. The main objective of these methods is to weaken the shock and reduce wave drag. Other passive control method is a bump. 2D bump leads to significant wave drag reduction, but also results in to high penalty under off-design conditions [3]. More recent studies were performed with 3D bumps to enhance the off-design performance [4].

There are also different passive and active methods to energize the boundary layer under shock foot to prevent flow separation. Vortex generators (VGs) are the most popular method for this purpose. Mechanical VGs were considered in [5-6] and show their effectiveness. The main disadvantage of this method is drag increase under cruise condition. Air-jet (fluidic) VGs and tangential jet blowing with position at 15% of the chord length to control SBLI were also considered in [5]. Other active methods for SBLI control are suction [7] and application of plasma actuators [8-9]. These devices for active flow control can be turned off during cruise regime and can be used in a closed-loop strategy to optimize flow control. Their disadvantages are additional equipment, complexity and weight.

Some of these devices were investigated as the buffet control means. Mechanical VGs were studied in [10]. Special mechanical trailing edge device (TED) which can change rear loading of an airfoil was also considered in [10]. Fluidic VGs (air-jet VGs) as well as fluidic TED (jet near the trailing edge normal to airfoil pressure side) were studied in [11]. It was shown that mechanical and fluidic VGs are able to delay buffet onset in the angle-of-attack domain by suppressing separation downstream of the shock. The effect of the fluidic TED was different, the separation was not suppressed. In this case, the buffet onset was not delayed in the angle-of-attack domain, but only in the lift domain.

In the present study, buffet control method by tangential jet blowing is investigated. The jet of compressed air is blown continuously from small slot nozzle tangentially to the wing upper surface in the region of shock location to reduce shock-induced separation. The problem is solved numerically. Numerical simulation of the flow over transonic supercritical airfoil with active flow control is carried out on the base of Reynolds averaged Navier-Stokes (RANS) equations for different regimes. Calculations of the effect of different jet locations and intensities are performed. Aerodynamic performance characteristics of an airfoil with and without jet blowing are estimated.

2. Problem statement

The present study is undertaken to prepare experimental investigations in TsAGI T-112 transonic wind tunnel (WT) and to characterize flow features over the wing model. T-112 WT has square test section 0.6x0.6 m^2, stagnation temperature is environmental temperature (T_0=293 K), stagnation pressure is atmospheric (p_0=101325 Pa). The wing model has 2D geometry with airfoil from one side wall to another side wall of T-112 WT. Supercritical airfoil P-184-15SR with thickness 15% and chord length c=0.2 m is chosen for investigations as a baseline configuration (Figure 1). Reynolds number based on free-stream parameters and chord length is Re=2.6×10^6.

Figure 1: Smooth airfoil P-184-15SR

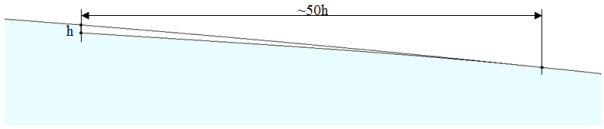

Figure 2: Slot geometry at X_i=0.6

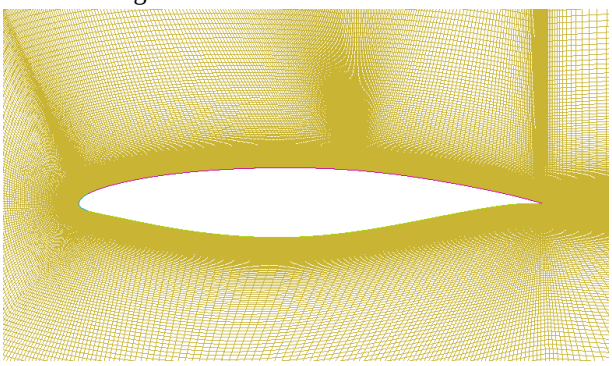

Figure 3: Grid near the airfoil

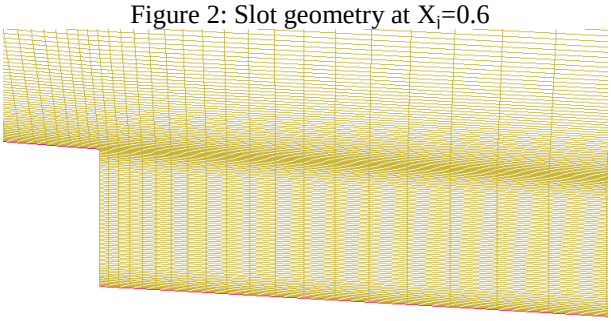

Figure 4: Grid near slot nozzle

The smooth airfoil and the airfoil with the slot nozzle for jet blowing on the upper surface are used. The slot position is X_j/c =0.55, 0.6, 0.65, where X is longitudinal distance. The height of the slot nozzle is h=0.15 mm. This slot is generated by removing small part of the airfoil as indicated in Figure 2.

2D RANS and unsteady RANS (URANS) simulations of the flow past the airfoil on transonic regimes are carried out to estimate aerodynamic performance characteristics. Structured hexahedral grid with C-H topology is used for numerical simulations (Figure 3). Far-field boundaries are placed 50 chords away from the airfoil. Two grids are used. The first grid is for the smooth airfoil and the second one is for the configuration with the slot nozzle. The size of the first cell in the direction normal to the slot nozzle equals to 0.01 mm (Figure 4). Typical grid with approximately 200000 nodes is shown in Figure 3. Grid nodes are clustered normal to the surface inside the boundary layer so that Y^+_1<1.

The calculations are carried out for the ideal compressible gas with laminar Prandtl number Pr=0.72. Laminar viscosity-temperature dependence is approximated by Sutherland law with Sutherland constant 110.4 K. Spalart-Allmaras (SA) or SST turbulence model are used for simulations.

The jet is simulated by boundary condition stated on the slot nozzle. One of the main jet parameters is jet momentum coefficient

$$C_\mu = \frac{Q_j V_j}{0.5\rho_\infty V_\infty^2 S}$$

where Q_j is jet mass flow rate, V_j is constant jet velocity at slot nozzle, ρ_∞ is free-stream density, V_∞ is free-stream velocity, S is wing area. Slightly supersonic jet (jet Mach number is $M_j = 1.24$) is realized for the value $C_\mu = 0.0043$.

Numerical solutions are obtained using an implicit finite-volume method. The equations are approximated by a second-order shock-capturing scheme. The flux vector is evaluated by an upwind flux-difference splitting of Roe. Second order upwind scheme is used for spatial discretization of convective terms. Central-differencing scheme is used for diffusion terms. An Euler implicit discretization in time is used for steady-state problem. The time marching is proceeded until a steady-state solution sets in.

Special RANS calculations are carried out to clarify sensitivity of the results to grid density. Figure 5 shows pressure coefficient (C_p) distribution along the chord for different grids. Several grids are considered: ~90000, ~200000, ~280000 and ~380000 grid nodes. For these cases, free-stream parameters are the following: M=0.725 (Mach number) and α=2° (angle of attack). Jet blowing parameters are X_j/c=0.6 and $C_\mu = 0.0043$. It should be noted that the grid with ~200000 is sufficient for investigations of jet blowing effect.

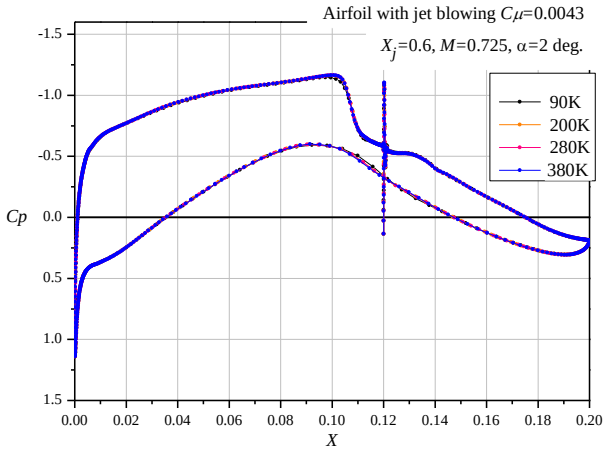

Figure 5: Pressure coefficient distributions along the chord for different grids; M=0.725, α=2°, X_j/c=0.6, C_μ = 0.0043

For unsteady problem (2D URANS), the second order time discretization is used. These calculations are performed with time step $\Delta t=2\times10^{-6}$ s. Dual time stepping scheme is used. Internal iterations are converged with error 10^{-6}. Calculations with $\Delta t=1\times10^{-6}$ s show that the results are independent on time step in this range.

3. 2D RANS simulations

In this section, P-184-15SR airfoil aerodynamics with tangential jet blowing is investigated by means of 2D RANS numerical simulations. SST turbulence model is used in this section. At high angles of attack, a steady state solution is not achieved. In this case, results are obtained by averaging during several periods of value oscillation. Amplitudes of oscillations are shown in figures by constrained markers.

Figures 6-7 show aerodynamic performance characteristics of the airfoil P-184-15SR with tangential jet blowing for M=0.725, X_j/c=0.6. Different jet intensities are considered: $C_\mu = 0.0021, 0.0046, 0.0068, 0.0086, 0.018$. For comparison, characteristics of smooth airfoil are plotted also. The value $C_\mu = 0.018$ seems to be very high. It should be noted that the lift and drag values are computed without taking into account slot nozzle.

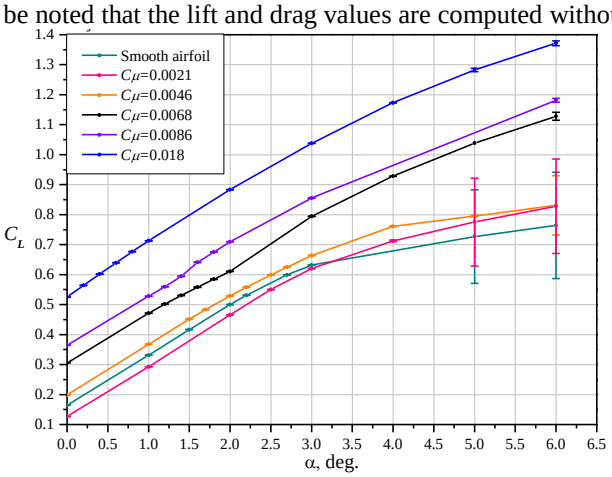

Figure 6: Lift coefficient versus angle of attack for different jet intensities, M=0.725, X_j/c=0.6

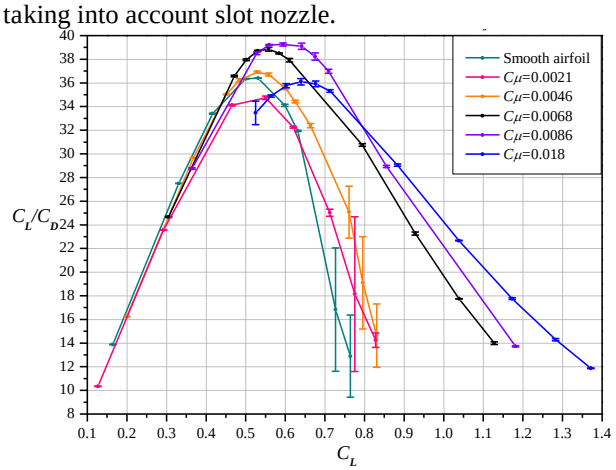

Figure 7: Lift to drag ratio for different jet intensities, M=0.725, X_j/c=0.6

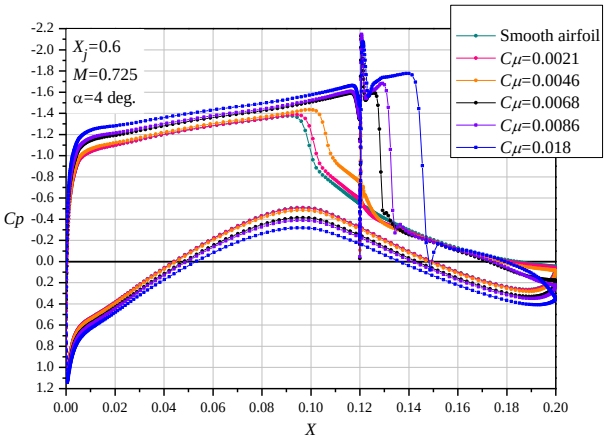

Figure 8: Pressure coefficient distributions for different jet intensities, M=0.725, X_j/c=0.6, α=4°

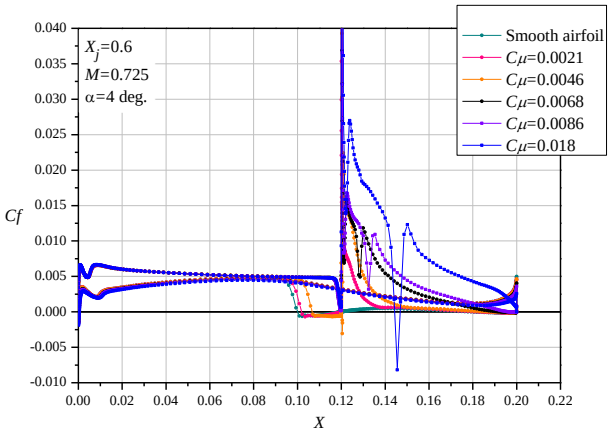

Figure 9: Friction coefficient distributions for different jet intensities, M=0.725, X_j/c=0.6, α=4°

It should be noted that lift increases while C_μ increases (Figure 6). Lift to drag ratio is maximal for the cases with $C_\mu = 0.0068$ and $C_\mu = 0.0086$. C_L with maximal lift to drag ratio increases while C_μ increases for $0.0046 \leq C_\mu \leq 0.0086$. Oscillations of C_L and C_D start to grow at higher C_L and AoA as it is indicated by constrained markers. Pressure and friction coefficient distributions are presented in Figures 8-9 for α=4° which is close to buffet regimes.
In these cases, the jet blowing (X_j/c=0.6) is located slightly downstream of the shock position (~55% of the chord) of the smooth airfoil. Jet blowing with relatively small intensities $C_\mu < 0.0068$ slightly moves the shock and shock position is still upstream of X_j. Jets with $C_\mu \geq 0.0068$ move the shock strongly and shock position is downstream of X_j. Mach number fields near slot nozzle for the cases of $C_\mu = 0.0046$ and $C_\mu = 0.0068$ are shown in Figure 10.

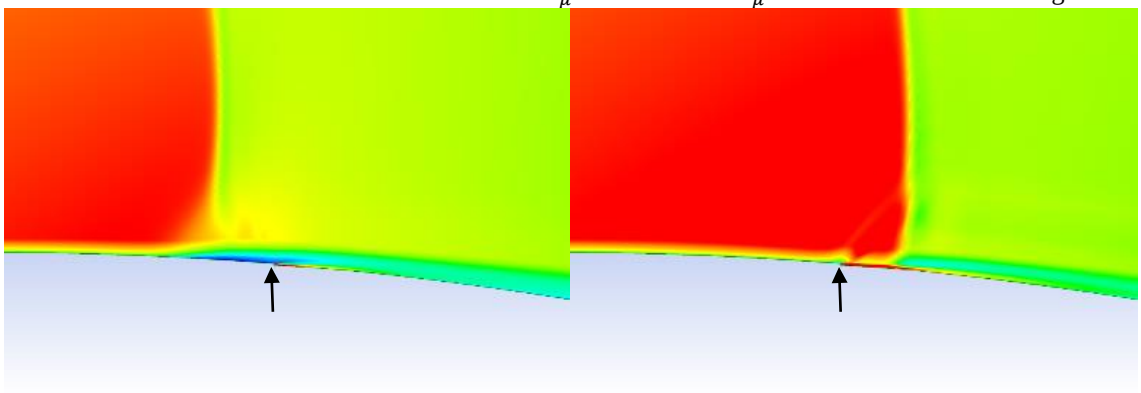

Figure 10: Mach number fields near slot nozzle, M=0.725, X_j/c=0.6, α=3°; arrow indicates slot nozzle location; left – $C_\mu = 0.0046$, right – $C_\mu = 0.0068$

The shock is stronger and wave drag increases while C_μ increases. Moreover, friction drag downstream of the shock increases while C_μ increases. There is a separation under the shock foot for the case of smooth airfoil and for the cases with $C_\mu < 0.0068$. For the cases with $C_\mu \geq 0.0068$ there is no separation under shock foot.
Additional calculations are performed to understand influence of slot location on aerodynamic characteristics. Results have been obtained for the slot with X_j/c=0.55, 0.6, 0.65. Figures 11-12 show aerodynamic performance characteristics for different X_j/c and M=0.725, $C_\mu = 0.0086$. Pressure coefficient distributions are presented in Figure 13 for M=0.725, α=4°.

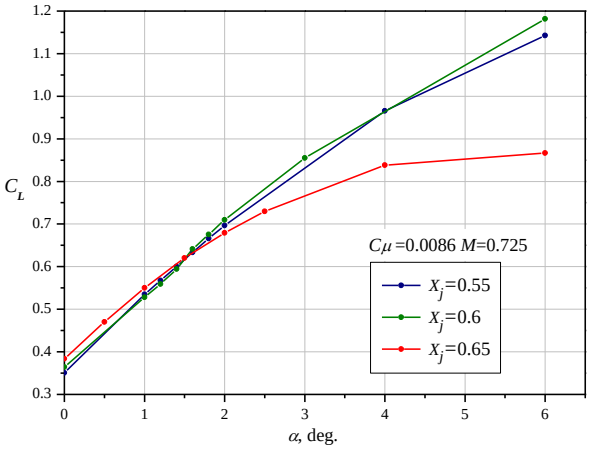

Figure 11: Lift coefficient versus angle of attack for different jet locations, M=0.725, $C_\mu = 0.0086$

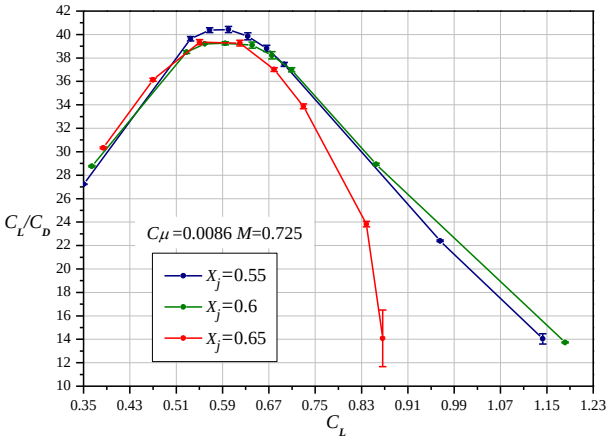

Figure 12: Lift to drag ratio for different jet locations, M=0.725, $C_\mu = 0.0086$

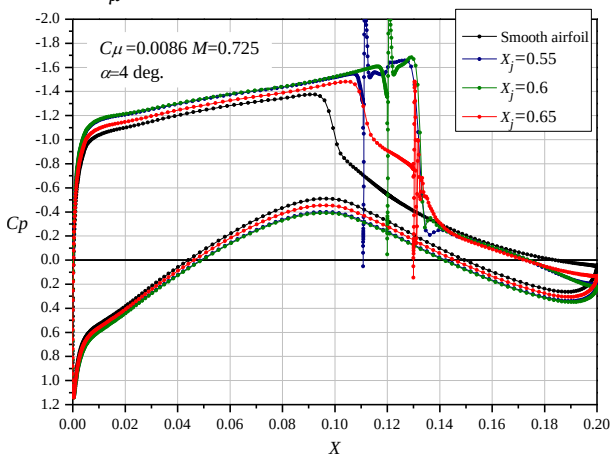

Figure 13: Pressure coefficient distributions for different jet locations, M=0.725, $C_\mu = 0.0086$, α=4°

It should be noted that the case with X_j/c=0.65 have lower lift properties than the other cases with X_j/c=0.55 and 0.6. In this case the position of the jet blowing is far downstream of the shock wave and the effect of jet blowing is weaker. The jet blowing with X_j/c=0.55-0.6 is most favorable.

4. 2D URANS simulations

Buffet characterization on the P-184-15SR airfoil on the base of 2D URANS studies are carried out for the cases without jet blowing. SA turbulence model is used in this section. Summary of these results on (M, α) plane is shown in Figure 14. Regimes below solid line correspond to regimes without buffet, while regimes under solid line correspond to buffet onset. C_L convergence history for the case M=0.73 and α=4° without buffet is shown in Figure 15a. The similar C_L convergence history for the case with buffet M=0.73 and α=4.5° is shown in Figure 15b.

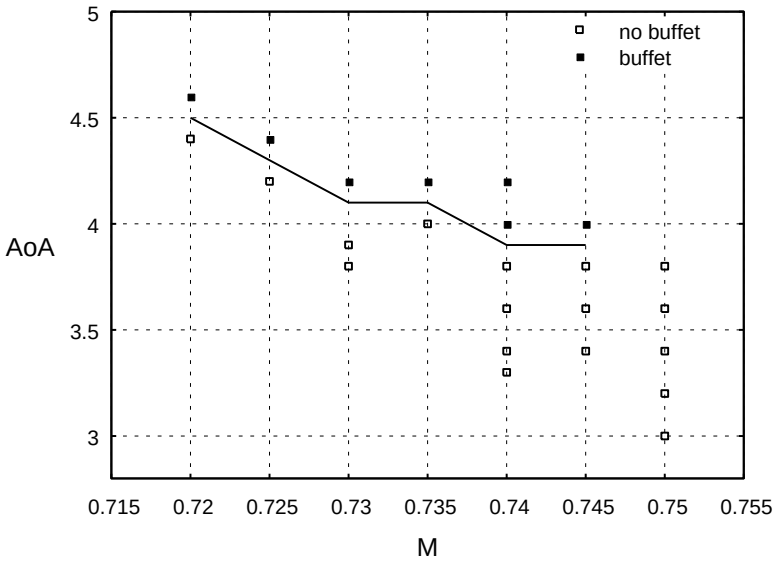

Figure 14: Buffet onset on (M, AoA) plane; regimes without jet blowing

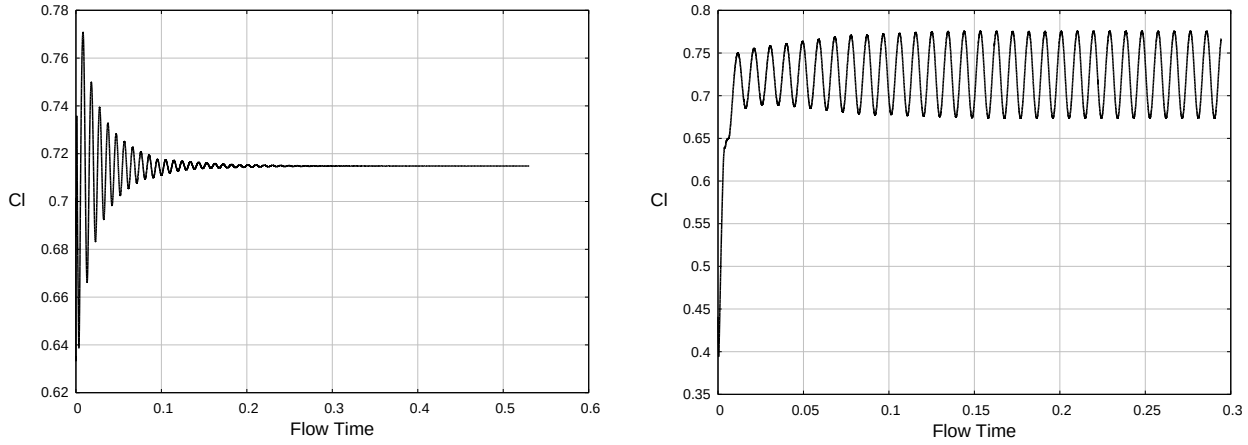

Figure 15: C_L convergence history for the case M=0.73, α=4° (a) and M=0.73, α=4.5° (b); time in seconds

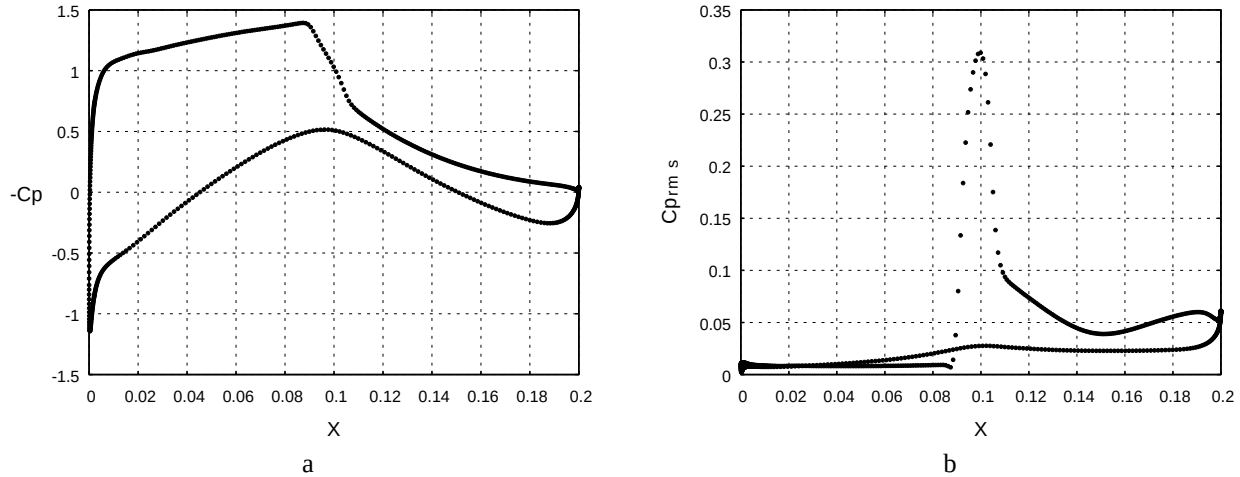

Figure 16: Time averaged wall C_p distribution (a) and RMS values of C_p (b) for the case M=0.73, α=4.5°

Mean (time averaged) wall C_p distribution for M=0.73, α=4.5° is shown in Figure 16a while root mean square (RMS) values of the wall C_p are shown in Figure 16b. Mach number field for this regime is shown in Figure 17 in different moments of buffet period. Frequency of the main buffet period is 106 Hz.

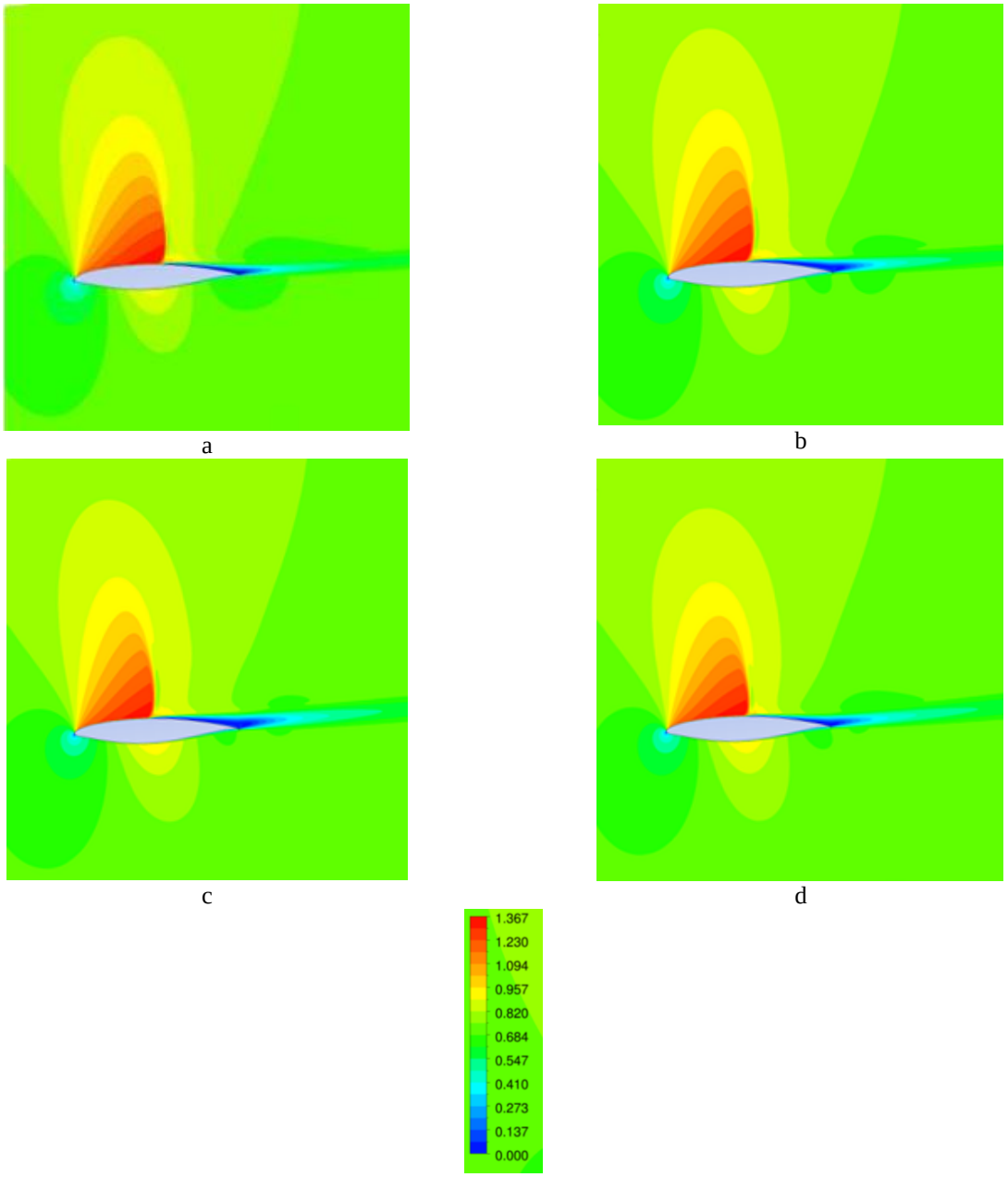

Figure 17: Mach number field for different moments of buffet period; a – initial, b – ¼ of period, c – ½ of period, d – ¾ of period

Lift curve for the case M=0.73 is shown in Figure 18. Brown curve corresponds to the case without blowing obtained by RANS simulations, while green curve corresponds to the case without blowing obtained by URANS simulations. Deviations of green curve designate RMS values. Both curves are close to each other. It should be noted that the deviation of lift curve from the linear regime is near α=2° while buffet onset regimes in URANS begin from α=4.2°. Orange curve of Figure 18 corresponds to the case of jet blowing with $C_\mu = 0.0086$ obtained by RANS simulations while blue curve corresponds to the case with jet blowing obtained by URANS simulations. Both curves are close to each other. There are no oscillations of C_L in the case with jet blowing and there is no buffet. One can conclude that tangential jet blowing delays buffet.

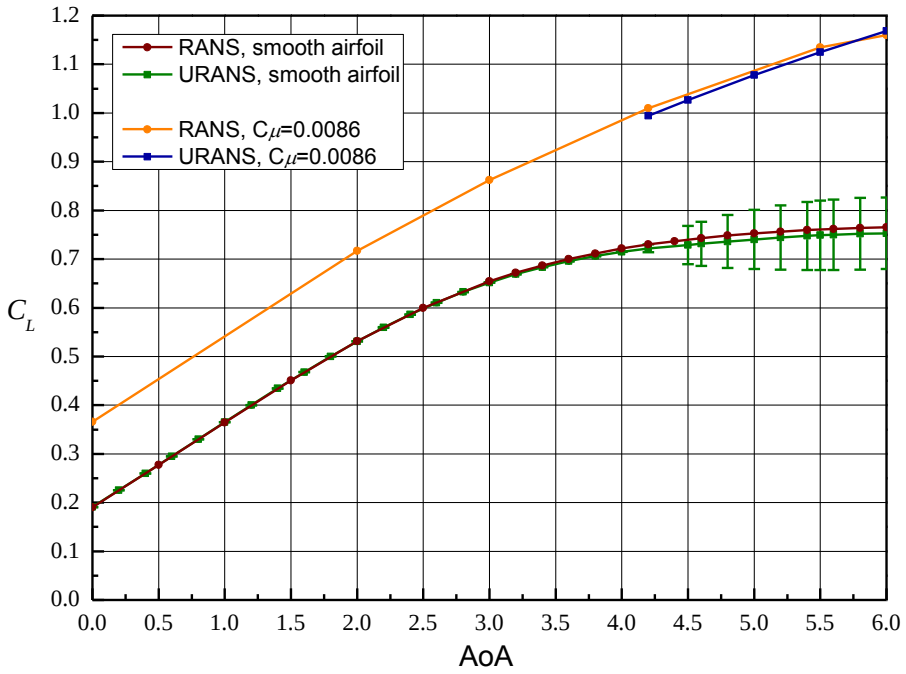

Figure 18: Lift curve for M=0.73 with and without tangential jet blowing

5. Summary

Two-dimensional numerical simulations are carried out to characterize the buffet phenomenon on transonic supercritical airfoil P-184-15SR with thickness 15% and chord length 200 mm. The problem is solved in the framework of Reynolds averaged Navier-Stokes equations. Steady-state (RANS) and unsteady (URANS) simulations are performed. Tangential jet blowing is investigated to delay buffet onset on the airfoil. In this case, the jet of compressed air is blown continuously from small slot nozzle (height is 0.15 mm) tangentially to wing upper surface in the region of shock location to reduce shock-induced separation.

Aerodynamic performance characteristics are estimated for M=0.72-0.75 and different angles of attack. Lift increases while C_μ increases. The range of $C_\mu = 0.006 - 0.009$ is the most favorable with jet location near shock foot X_j/c=0.55-0.6. For the cases with $C_\mu \geq 0.0068$ jet blowing suppresses separation under shock foot. In the case of jet blowing, wave drag and friction drag downstream of the shock increase while C_μ increases. Nevertheless, for high AoA, drag for the constant lift decreases with increase of C_μ (if the lift and drag values are computed without taking into account slot nozzle).

2D RANS and URANS simulations show that the jet blowing leads to the increase of C_L or AoA at which solutions start to oscillate. One can conclude that tangential jet blowing delays buffet onset.

Authors thank to K.G. Khayrullin for the help in numerical simulations.
This work is supported by BUTERFLI Project of the 7th Framework Program of the European Commission (Grant Agreement 605605).

References

[1] Bahi, L., Ross, J.M., and Nagamatsu, T. 1983. Passive shock wave/boundary layer control for transonic airfoil drag reduction. AIAA Paper 1983-0137.

[2] Raghunathan, S. 1988. Passive control of shock-boundary layer interaction. *Progress in Aerospace Science*. 25: 271-296.

[3] Birkemeyer, J., Rosemann, H., and Stanewsky, E. 2000. Shock Control on a Swept Wing. *Aerospace Science and Technology*. 4:147-156.

[4] Ogawa, H., Babinsky, H., Patzold, M., and Lutz, T. 2008. Shock-Wave/Boundary-Layer Interaction Control Using Three-Dimensional Bumps for Transonic Wings. *AIAA Journal*. 46(6):1442-1452.

[5] Pearcey, H.H. 1961. Shock-induced separation and it's prevention by design and boundary layer control. In: *Boundary layer and flow control – it's principles and application*. Ed. by Lachmann.Vol. 2. London. Pergamon Press. 1170-1361.
[6] Gadetskiy, V.M., Serebriyskiy, Ya.M., and Fomin, V.M. 1974. Investigation of the influence of vortex generators on turbulent boundary layer separation. NASA TT F-16056.
[7] Krogmann, P., Stanewsky, E., and Thiede, P. 1985. Effects of suction on shock/boundary layer interaction and shock-induced separation. *J. Aircraft*. 22(1): 37-42.
[8] Leonov, S.B., Yarantsev, D.A., Gromov, V.G., and Kuriachy, A.P. 2005. Mechanisms of Flow Control by Near-Surface Electrical Discharge Generation. AIAA 2005-780.
[9] Marino, A., Catalano, P., Marongiu, C., Peschke, P., Hollenstein, C., and Donelli, R. 2013. Effect of High Voltage Pulsed DBD Plasma on the Aerodynamic Performances in Subsonic and Transonic Conditions. AIAA 2013-2752.
[10] Caruana, D., Mignosi, A., Robitaille, C., and Correge, M. 2003. Separated Flow and Buffeting Control. *Flow, Turbulence and Combustion*. 71: 221-245.
[11] Dandois, J., Molton, P., Lepage, A., Geeraert, A., Brunet, V., Dor, J.-B., and Coustols, E. 2013. Buffet Characterization and Control for Turbulent Wings. *Aerospace Lab Journal*. 6: AL06-01.